Production of multiparticle final states by coherent excitation of projectiles in nuclear targets*

Paul M. Fishbane
Institute for Theoretical Physics, State University of New York at Stony Brook, Stony Brook, New York 11790 and Physics Department, University of Virginia, Charlottesville, Virginia 22901 †

J. S. Trefil
Physics Department, University of Virginia, Charlottesville, Virginia 22901
(Received 19 June 1973)

The production of multiparticle final states on nuclear targets via multiple coherent excitation of the projectile is developed. By coherent excitation we mean that class of production models including fragmentation models or diffractive excitation models. It is found that both the rapidity distribution of secondaries in inclusive reactions and the multiplicities can be calculated, and new features of the excitation models are revealed. The calculable quantities are found to depend only weakly on the atomic number of the target; in particular, the single-particle distribution in the target fragmentation region grows roughly as $A^{1/4}$. An amusing possibility of boosting effective beam energy for resonance production by using nuclear targets emerges.

I. INTRODUCTION

The idea that we can learn a great deal from the study of the production of multiparticle final states on nuclear targets has been put forward many times.[1,2] The general approach is to point out that in production on a nucleus the multiparticle final state can interact with downstream nucleons in that nucleus, so that relatively direct knowledge of its interactions can be obtained. Such knowledge is not, of course, obtainable from the use of conventional hydrogen targets.

Previous proposals[3] along these lines have been primarily concerned with the properties of the final-state particle *per se* (for example, with the determination of unstable particle-nucleon cross sections) and hence have been involved primarily with coherent reactions on nuclei. We intend to concentrate instead on the complementary problem of using the nucleus to investigate the production mechanism itself, rather than the properties of the final state, and hence will discuss only incoherent nuclear reactions.

In general, we can think of current models for multiparticle production and inclusive reactions as falling into two general classes: coherent-production models (CPM), in which the final state results as a decay of some long-lived excited intermediate state (such as a "fireball"), and the incoherent-production models (IPM), in which the particles in the final state appear without the presence of any long-lived intermediate excited state. Examples of CPM might be diffractive excitation,[4] nova,[5] or fragmentation[6] models, while examples of IPM might include multiperipheral[7] or dual resonance[8] models. It is obvious that in the case of the IPM, any of the particles which are produced in the first inelastic collision in a nucleus can initiate another inelastic collision downstream, thereby setting up an intranuclear cascade. In CPM, on the other hand, such cascades will not develop so long as the lifetime is greater than a nuclear radius. In Refs. 1 and 2, CPM were treated by assuming that the intermediate "fireball" would leave the nucleus unscathed except for possible elastic scatterings. This difference between the two classes of models was the basis for the claim that a study of nuclear production could provide information about the multiparticle production process.

In a recent series of papers,[9-11] the authors have extended the Glauber theory for inclusive reactions on nuclei to the problem of the development of the intranuclear cascade corresponding to pure IPM production on the nucleons. In this note, we do the same for the CPM, taking into account the fragmentation of downstream nucleons by the "fireball" and the possibility of further excitation of the fireball itself. Our aim is to provide the best possible theoretical predictions for the inclusive nuclear reaction, so that when experiments of this type are completed clear statements about the nature of multiparticle final states will be possible.

Accelerator experiments of this type are, of course, very desirable, but it should also be noted that in order to test asymptotic concepts such as scaling it will be immensely helpful to go to cosmic-ray data to get meaningful increases in energy. Because of the relative scarcity of cosmic rays of the highest energies, nuclear targets are used routinely in cosmic-ray work, either as

emulsions or in measuring reactions in the atmosphere itself. Thus, a further motivation for our work is that adequate description of particle-nucleus production processes will enable us to interpret[12,13] high-energy cosmic-ray data as well as lower-energy accelerator data. We expect that rules for distinguishing IPM and CPM will not be the only result of our work.

Finally, the authors feel that the particle-nucleus interaction forms a useful theoretical laboratory in which to study scaling in composite systems, since we are dealing with a composite system (the nucleus) whose properties are well known (a benefit which we do not enjoy in working with partons or quarks, for example).

With this motivation, we turn to the problem of describing nuclear processes involving the CPM. In Sec. II we work out the kinematics of multistep processes, deriving some results which could also be applied to simple high-mass resonance production as well as to inclusive reactions. In Sec. III we discuss various models for the interactions of "fireballs" with nuclei, while in Sec. IV we describe the general inclusive nuclear process in the CPM picture. In Sec. V we discuss nuclear scattering weights on actual nuclei, using the multistep incoherent formalism developed previously,[14] and finally in Sec. VI we present some distributions and multiplicity results.

II. EXCLUSIVE SCATTERING: MASS BUILDUP IN RESONANCE PRODUCTION

Coherent-production models all involve the formation of hadronic resonances in one form or another. Moreover, the production and study of hadronic resonances *per se* has always been one of the primary interests of high-energy physics. The possibility of using nuclear targets to study such properties of the resonant state as its elastic cross section (e.g., in ρ photoproduction) has of course been widely discussed elsewhere.[3] Therefore in this section we restrict our attention to some very simple kinematic aspects of resonant production on nuclear targets. We shall in particular show that for an incident beam of given energy it is possible to produce resonant states of much higher mass than is possible on a hydrogen target. This statement is independent of the Fermi motion of the nucleons (which can itself be used to boost the effective energy of the incident beam). Our results depend only on the kinematics of the multiple scattering process, which, as we shall see, converts the available s in a reaction from that appropriate to a nucleon to that appropriate to a target with up to A nucleons. While this general idea has been discussed previously,[15] to our knowledge the detailed kinematics has not appeared in the literature until now. The possible use of rescattering in nuclei to build up discrete quantum numbers in final states has been discussed previously.[14]

The results of this section could therefore be applied to processes in which high-mass resonances are to be produced from beams whose energy is insufficient to produce the desired final state from hydrogen targets alone. We shall, of course, also use the results in our studies of inclusive reactions in subsequent sections.

Suppose that we consider the two-body collision $1+2\to 3+4$, where particle 2 is a constituent of the composite system and we consider particle 3 as an excitation of the projectile 1. Let $s^{(1)}=(p_1+p_2)^2$ be available in this initial collision. In a kinematic extreme of this collision, these particles are at rest in the center-of-mass frame, so so that $(m_3+m_4)^2=s^{(1)}$. We assign the individual excitations 3 and 4 a fractional division x_1 of the momentum,

$$m_3=x_1(s^{(1)})^{1/2},\quad m_4=(1-x_1)(s^{(1)})^{1/2}. \tag{2.1}$$

In this limit, the momentum transfer in the initial collision is

$$\begin{aligned} t^{(1)}&=(p_1-p_3)^2\\ &=s^{(1)}x_1(x_1-1)+m_1^2(1-x_1)+m_2^2x_1. \end{aligned}\tag{2.2}$$

By computing the energy E_3 of the initial excitation in the laboratory frame, one can find $s\approx s^{(2)}$ available for a second collision of particle 3 on constituents of mass m_2, as in Fig. 1; the second collision produces particles 5 and 6. We have

$$\begin{aligned} s^{(2)}&=m_2^2+m_3^2-m_1^2-m_4^2+s^{(1)}+t^{(1)}\\ &=s^{(1)}x_1(1+x_1)+m_2^2(1+x_1)-m_1^2x_1. \end{aligned}\tag{2.3}$$

Note that for large $s^{(1)}$ if $x_1=1$, so that the projectile is excited to its kinematic limit, then

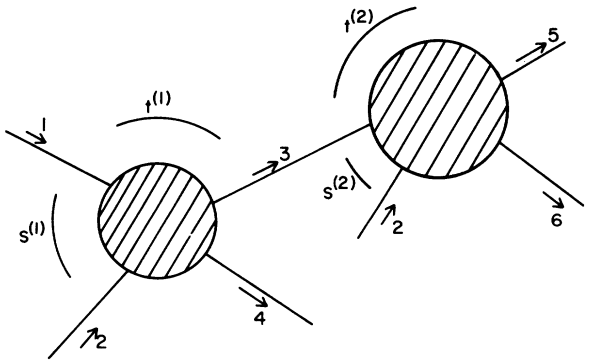

FIG. 1. Labeling of kinematic variables for two successive collisions: $1+2\to 3+4$ and then $3+2\to 5+6$.

$s^{(2)} \approx 2\,s^{(1)}$; thus the s available for the second collision has been doubled. Only if $x_1(1+x_1) > 1$ do we have $s^{(2)} > s^{(1)}$ so that a buildup is effected. For $s^{(i)} \gg m_1^2, m_2^2$, the boundary of this region, determined by $x_1(1+x_1) = 1$, is given by $x_1 = \frac{1}{2}(-1+\sqrt{5})$, which is just the first Fibonacci number, associated with the golden mean.[16]

We can now determine the energy variable $s^{(3)}$ available for scattering of particle 5 on another target 2. If we write

$$m_5 = x_2(s^{(2)})^{1/2}, \quad m_6 = (1-x_2)(s^{(2)})^{1/2}, \tag{2.4}$$

then ignoring m_1^2 and m_2^2 terms

$$\begin{aligned} s^{(3)} &\approx s^{(2)} x_2(1+x_2) - m_3^2 x_2 \\ &= s^{(1)}[x_1(1+x_1)\,x_2(1+x_2) - x_1^2 x_2]. \end{aligned} \tag{2.5}$$

This result can easily be generalized to the energy variable $s^{(n)}$ available for an nth collision on a target of (finite) mass m_2,

$$\begin{aligned} s^{(n)} = s^{(1)}\, &x_1(1+x_1)\cdots x_{n-3}(1+x_{n-3}) \\ &\times \{x_{n-2}(1+x_{n-2})x_{n-1}(1+x_{n-1}) - x_{n-1}x_{n-2}^2\}. \end{aligned} \tag{2.6}$$

By taking $x_1 = x_2 = \cdots = x_{n-1} = 1$, so that the projectile is excited to its kinematic limit in each successive collision, we find

$$s^{(n)} \xrightarrow[\{x_i\}\to 1]{} \begin{cases} 2s^{(1)}, & n=2 \\ 3\times 2^{n-3} s^{(1)}, & n>2. \end{cases} \tag{2.7}$$

This allows us a healthy increase on $s^{(n)}$. Break-even points on the $s^{(i)}$ of successive collisions are easily computed.

To complete the picture, we can also express the momentum transfer for the nth collision in terms of $s^{(1)}$ and the x_i. Ignoring m_2^2 terms,

$$t^{(n)} \approx x_n(x_n - 1)s^{(n)} + x_n^2(1-x_n)s^{(n-1)}. \tag{2.8}$$

We further note that the projectile excitation mass m_{2n+1} resulting from the nth collision is

$$m_{2n+1} = x_n(s^{(n)})^{1/2}. \tag{2.9}$$

Setting all the $x_i = 1$ maximizes m_{2n+1} at its kinematic limit,

$$m_{2n+1}^{\max} = \begin{cases} (s^{(1)})^{1/2}, & n=1 \\ (2s^{(1)})^{1/2}, & n=2 \\ (3\times 2^{2n-1} s^{(1)})^{1/2}, & n>2. \end{cases} \tag{2.10}$$

III. EXCITATION SPECTRUM IN ELEMENTARY COLLISIONS

In this section we will discuss the reactions which take place on individual nucleons in a multistep process. We can think of the initial projectile as being excited by an initial collision to a state of mass m_3 from an initial mass m_1, with a mass spectrum for inelastic collisions $\rho_1(m_3, m_1)$, in accordance with the notation of Sec. II.

We can make some very general statements about the form of ρ_1. First, ρ_1 should be nonzero for m from m_0 to the kinematic limit $\sqrt{s}$. In addition, in order to produce a pion multiplicity which grows as ln$s$, ρ_1 must fall as $1/m_3^2$ at large m_3.

A function which fits these requirements was suggested by Jacob and Slansky[5]:

$$\begin{aligned} \rho_1(m_3, m_1) &= \beta \exp\left(\frac{\beta}{\sqrt{s}} - \frac{\beta}{m_3 - m_1}\right) \Big/ (m_3 - m_1)^2 \\ &\underset{s\to\infty}{\approx} \beta \exp\left(-\frac{\beta}{m_3 - m_1}\right) \Big/ \ (m_3 - m_1)^2; \end{aligned} \tag{3.1}$$

ρ_1 is normalized to 1, with a maximum at $m_3 - m_1 = \frac{1}{2}\beta$.

The distribution ρ_1 is formed of the superposition of many resonances, which are thought to decay by stepwise cascade. Thus resonances at higher m_3 produce more stable particles ("pions"). If n is the number of produced pions,

$$n(m_3) = c(m_3 - m_1). \tag{3.2}$$

This allows us to compute the average pion multiplicity,

$$\langle n \rangle = \int_{m_t}^{\sqrt{s}} dm_3 \rho_1(m_3, m_1)\, n(m_3) \underset{s\to\infty}{\sim} \tfrac{1}{2} c\beta \ln s, \tag{3.3}$$

the logarithmic term arising from the region of ρ_1 which is $\sim (m_3 - m_1)^{-2}$.

When we turn to the problem of dealing with a nuclear process involving the formation of these excitations, however, a new problem develops. Basically, this is because the mass spectrum $\rho_1(m_3, m_1)$ describes the excitation of an incident stable particle mass m_1, and hence could be used to describe the first inelastic collision in a multistep process. In subsequent collisions, however, the incident particle is itself an excitation from a previous collision.

There are two reasonable models for the spectrum resulting from such a collision, and we shall consider them in turn after some preliminary work is carried out. Let us call the secondary spectrum $\rho'(m_5, m_3)$, where m_3 lies within the spectrum of a primary excitation $\rho_1(m_3, m_1)$. In general we expect that m_5 can run from m_1 (i.e., a deexcitation of the projectile) up to $\sqrt{2s}$ [as in Eq. (2.10)]. In addition we expect that $\rho'(m_5, m_3)$

$\sim m_5^{-2}$ for large values of m_5, where ρ' should be similar to ρ_1.

The measured mass spectrum after two collisions will then be

$$\rho_2(m_5, m_1) = \int_{m_i}^{\sqrt{s}} dm_3 \rho'(m_5, m_3) \rho_1(m_3, m_1) . \tag{3.4}$$

ρ_2 will be normalized to unity when ρ_1 and ρ' are. In addition, $\rho_2 \sim m_5^{-2}$ for large values of m_5, so that the logarithmic growth in multiplicity will be retained.

These expressions are easily generalized. After N collisions the measured distribution will be given recursively as

$$\rho_N(m_{2N+1}, m_1) = \int_{m_1}^{m_{2N-1}^{\max}} dm_{2N-1} \rho'(m_{2N+1}, m_{2N-1}) \times \rho_{N-1}(m_{2N-1}, m_1), \tag{3.5}$$

which will remain normalized. This spectrum also falls as $1/m_{2N+1}^2$, so that logarithmic growth of multiplicity remains. The $\ln s$ terms now get an additional additive contribution from the increased upper limit of m_{2N+1}, as in Eq. (2.10). In particular, for $N > 2$,

$$\langle n \rangle_N \sim \int^{m_{2N+1}^{\max}} \frac{dm}{m} \sim \ln[(3\times 2^{2N-1} s)^{1/2}] \sim \tfrac{1}{2}[\ln s + \ln(3\times 2^{2N-1})], \tag{3.6}$$

where $\langle n \rangle_N$ is the average number of produced (projectile) pions after exactly N collisions.

As a final general remark we may speculate on the properties of ρ_N as N becomes large. One would not expect a systematic effect on ρ_N as N increases other than the kinematic change in its limit. It is very tempting to go one step further and say that after many collisions the excitation spectrum reaches an equilibrium which is completely independent of the original projectile. This spectrum would then become just a universal function for all projectiles, i.e., pions, protons, etc. We shall discuss in the next section experimental tests of this idea.

We now turn to discussion of models.

Model I. In this model the production of m_5 "remembers" the initiating mass m_3, and ρ' is taken to have a maximum at $m_5 = m_3$. Thus, for example, a propagating $N'(1470)$ which is the excitation of a nucleon would prefer to scatter elastically rather than make a transition back to a nucleon in a second collision. A possible form for ρ' might be

$$\rho'(m_{2N+1}, m_{2N-1}) = C \exp\left(\frac{-a}{m_{2N+1} - m_1}\right) \times \frac{1}{(m_{2N+1} - m_{2N-1})^2 + \Gamma^2} , \tag{3.7}$$

where C is a normalization constant and Γ is some width parameter for the spectrum (not to be confused with a resonance decay width).

Model II. One may argue that the incoming excitation of mass m_3 and its own excitation of mass m_5 are each "complicated" systems in a quantum-mechanical sense, as opposed to the stable configuration of mass m_1 or of other low masses. We might then say that the overlap of two complicated systems (e.g., of m_5 with m_3) is in general much smaller than the overlap of a complicated system with a simple system (e.g., of m_5 with low masses). This is an argument for taking ρ' to be basically similar to the initial distribution ρ_1, save that the upper limit on ρ' should be adjusted to its appropriate kinematic limit,

$$\rho'(m_{2N+1}, m_{2N-1}) = \rho_1(m_{2N+1}, m_1; N) . \tag{3.8}$$

We have added the argument N on ρ to indicate that its kinematic upper limit for m_{2N+1} is not $(s^{(1)})^{1/2}$ but instead is given according to Eq. (2.10) by $(3\times 2^{2N-1} s^{(1)})^{1/2}$ for $N > 2$.

While we do not feel strongly impelled to choose either model on theoretical grounds, a task which for the present we can leave to experiment, model II does have the advantage that various integrals, etc. are more tractable. Therefore for purposes of exposition we use this model throughout the remainder of this paper.

In particular, we have from Eq. (3.5) the distribution after N collisions

$$\rho_N(m_{2N+1}, m_1) = \rho_1(m_{2N+1}, m_1; N) , \tag{3.9}$$

and from Eq. (3.6) the multiplicity after N collisions ($N > 2$)

$$\langle n \rangle_N \underset{s\to\infty}{\sim} C\beta \ln(3\times 2^{2N-1} s^{(1)})^{1/2} . \tag{3.10}$$

It is important to note, however, that an extra assumption has been introduced into our work at this point. Such an assumption was not necessary in considering the intranuclear cascade in the IPM results, since in that case downstream reaction is initiated by a pion or some other elementary particle whose cross section for a given final state can be independently measured.

IV. INCLUSIVE SCATTERING: GENERAL PROPERTIES

In order to explore the features of inclusive scattering on nuclear targets when an incoherent production process is the primary dyamical model, no assumptions were required beyond those already given by the model. By contrast, when the primary model is a coherent model we require one additional assumption for the qualitative discussion and still another assumption for more detailed quantitative calculations. These assumptions are, respectively, the following.

(i) The lifetime of the projectile excitation which propagates through the nucleus is greater than the time required to cross the nucleus. This means that the excitation must have a lifetime comparable to (or greater than) the ordinary low-mass hadronic resonances, i.e., $\tau = O(10^{-23}$ sec). This last statement provides the main support for this assumption, since, as discussed in Sec. III, the excitation is regarded in some sense as a superposition of hadronic resonances.

(ii) The cross section of the projectile excitation for further collisions with nucleons is comparable to the known hadronic cross sections. The main argument for this is again given by the fact that where low-mass resonance cross sections have been measured in nuclear scattering experiments, their cross sections have been in the range of tens of mb, i.e., typically hadronic.[17] We emphasize that, while we have included this assumption here for completeness, only assumption (i) is required for the general properties we are discussing in this section.

The qualitative picture of the scattering process is shown in Fig. 2. The projectile proceeds through the nucleus, reaching a new stage of excitation with each inelastic collision. After N collisions it leaves the nucleus, with an excitation spectrum $\rho_N^{\text{proj}}(m_{2N+1}, m_1)$. It then decays, giving an inclusive distribution characteristic of ρ_N^{proj} in the rapidity region characteristic of the projectile (i.e., the Feynman variable $x > 0$). In the case of model II described in Sec. III, this will take the form of the projectile distribution in the primary collision.

While the projectile excitation proceeds through the nucleus, it produces a target excitation characteristic of a target nucleon for each inelastic collision. (We continue to assume the factorization property, so that the target excitation is independent of the projectile.) Thus when there are N collisions, there are N target excitations. These N excitations then begin to decay, producing (see below) a single-particle inclusive distribution in the target rapidity region (i.e., $x < 0$) equal to N times a single-target nucleon distribution. We should note at this point that, plotted as a function of the Feynman variable x for projectile-nucleus scattering, the distribution for $x < 0$ will be N times the nucleon distribution as seen in projectile-nucleon scattering but compressed into the region $-A^{-1} < x < 0$ rather than $-1 < x < 0$. This is because each nucleon carries only A^{-1} of the nucleus' center-of-mass momentum.[10]

The target excitations range from those nearly at rest in the nucleus (in the target-fragmentation region) to those moving relatively fast (near $x = 0$). The latter come from the high-mass excitations producing many pions. We would argue that the low-velocity excitations produce an observed single-particle distribution not very different from N times a target-nucleon distribution because the slow stepwise decay never produces very energetic particles relative to the nucleus *within* the nucleus; these low-energy products either leave the nucleus by elastic-scattering propagation or are actually produced outside the nucleus when the decaying excitation diffuses out of the nucleus before its decay process is completed. On the other hand, a high-mass target excitation may be moving fast enough relative to the remainder of the target to itself have significant inelastic collisions. This will then contribute to a blurring or smoothing of the observed distribution. Numerical calculations of such effects are in the general class of final-state interactions and are ignored in the present work. Note also that there are no scale-breaking effects in this description, in contrast with the incoherent-production-process case. Thus the inclusive distribution from a nuclear reaction will scale when the primary distribution does.

On the average, N will be given by the number of mean free paths in the nucleus for inelastic collision.[1,14] Thus the height of the target distribution will grow as $A^{1/3}$. This also suggests that a test of the equilibrium hypothesis of the previous sec-

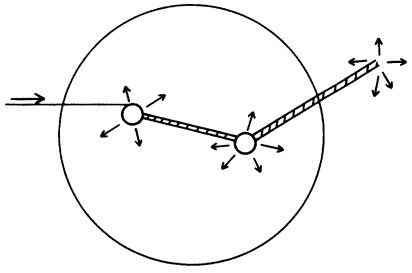

FIG. 2. Qualitative picture of inelastic nuclear scattering. The projectile proceeds through the nucleus, undergoing excitation and at the same time exciting target nucleons. The projectile excitations do not decay within the nucleus.

tion is the growing independence of the $x>0$ distribution form the nature of the incoming projectile as A increases.

This optical approximation for the propagation through the nucleus is in fact only good when a single particle (in this case, the excitation) propagates through the nucleus. Mean-free-path approximations fail badly when many particles propagate through the nucleus, as in incoherent production processes. (See Refs. 9 and 18.)

If we are to proceed from this point, it is necessary to describe the primary collision further. Figure 3 shows that the primary collision can be (a) single-projectile excitation, (b) simple target excitation, or (c) double excitation, with respective (constant) probabilities P, Q, and $R=1-P-Q$. In accordance with assumption (ii), we take P, Q, and R to be the same for an excitation-induced reaction as for the primary induced reaction. In N inelastic collisions within a nucleus, the probability $\mathcal{P}^N_{p,q,r}$ of p of type (a), q of type (b), and r of type (c), $N=p+q+r$, is

$$\mathcal{P}^N_{p,q,r}=\frac{N!}{p!\,q!\,r!}P^pQ^qR^r. \tag{4.1}$$

The average number $\langle \mathfrak{N}_P\rangle_N$ of collisions of type P is

$$\langle \mathfrak{N}_P\rangle_N = NP, \tag{4.2}$$

etc. Let the single-particle distribution of a target excitation be τ^{target} and let the single distribution of a projectile excitation characteristic of M successive collisions be τ^{proj}_M. Then the single-particle distribution from exactly N inelastic collisions in a nucleus would be

$$\tau = N(Q+R)\,\tau^{\text{nucleon}} + \tau^{\text{projectile}}_{\langle \mathfrak{N}_P\rangle_N+\langle \mathfrak{N}_R\rangle_N}. \tag{4.3}$$

In the model where the projectile excitation spectrum for M collisions is just the spectrum for one collision save for the upper limit, then essentially $\tau^{\text{projectile}}_M \to \tau^{\text{projectile}}_I$.

Finally, we must average over N. Let σ^A_N be the cross section for N inelastic collisions and any number of elastic collisions in a nucleus A. (We discuss this quantity in more detail in Sec. V.) Then the average number $\langle\langle \mathfrak{N}_P\rangle\rangle_A$ of P-type collisions is

$$\langle\langle \mathfrak{N}_P\rangle\rangle = \sum_{N=0}^{\infty}\sigma^A_N\langle \mathfrak{N}_P\rangle_N \Big/ \sum_{N=0}^{\infty}\sigma^A_N = P\sum N\sigma^A_N \Big/ \sum\sigma^A_N \approx P\langle N\rangle_A, \tag{4.4}$$

etc. This gives for the observed single-particle distribution

$$\tau = \langle N\rangle_A\,(Q+R)\,\tau^{\text{nucleon}} + \tau^{\text{projectile}}_{\langle N\rangle_A(P+R)}. \tag{4.5}$$

We conclude this section with values for P, Q, and R. These quantities were studied by the authors of Ref. 5 for π-p scattering, which is the case of primary interest to us; they found $P\approx 0.4$, $Q\approx 0.4$, and $R\approx 0.2$. We now need only to determine $\langle N\rangle_A$ to complete the picture.

V. NUCLEAR SCATTERING WEIGHTS

In this section we study σ^A_N, the cross section for exactly N inelastic collisions in a nucleus of size A. This quantity was of importance for the study of the observed single-particle distributions on nuclear targets, as discussed in the previous section. For simplicity, we take the inelastic cross section σ_{in} of all hadrons (i.e., of both the incident projectile and its entire excitation spectrum) to be the same. The computations of this section can easily be done with any values for the inelastic cross sections, but since we do not know the values of the excitation cross sections, it is economical to simply take one value. [If all the cross sections are constant and if scaling is observed in nuclear scattering experiments so that a coherent rather than incoherent production process is deduced to be dominant, then further nuclear scattering experiments and further calcula-

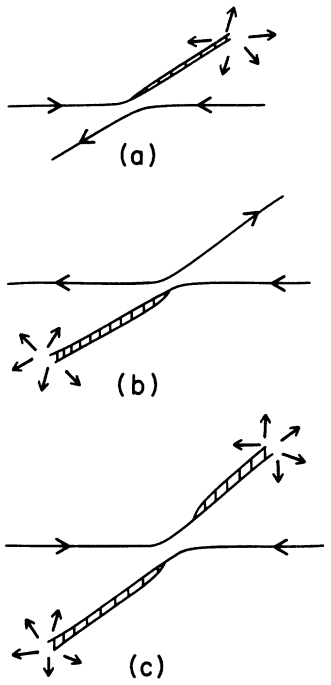

FIG. 3. Three types of excitation: (a) simple projectile excitation, (b) simple target excitation, (c) double excitation.

tions can be combined to measure the excitation cross sections.]

To calculate the σ_N^A, we rely heavily on the previous work of Trefil and von Hippel,[14] and we refer the interested reader there (see especially Sec. V) for more detail. We have in the optical approximation

$$\sigma_N^A = 2\pi \int_0^\infty B\, dB\, \frac{1}{N!}[t(B)]^N e^{-t(B)}, \tag{5.1}$$

where the weighted nuclear thickness $t(B)$ is

$$t(B) = A\,\sigma_{in} \int dz\, \rho(B, z), \tag{5.2}$$

and we take the (normalized) nuclear density function $\rho(B, z)$ as a Gaussian form,

$$\rho(B, z) = \left(\frac{1}{\sqrt{\pi}\,R}\right)^3 \exp\left(-\frac{B^2 + z^2}{R^2}\right). \tag{5.3}$$

The radius parameter R of this Gaussian distribution is taken from the root-mean-square radius $\langle r_{rms}\rangle$ of electron scattering experiments,

$$R = (\tfrac{2}{3})^{1/2}\langle r_{rms}\rangle\,. \tag{5.4}$$

If we insert Eq. (5.3) into (5.2), the z integration can be explicitly done, giving

$$t(B) = \frac{A\sigma_{in}}{\pi R^2} \exp\left(-\frac{B^2}{R^2}\right). \tag{5.5}$$

Inserting Eq. (5.5) in turn into Eq. (5.1), we can recognize an incomplete γ function $\gamma(n, x)$,

$$\gamma(n, x) = x^n \int_0^\infty d\alpha \exp(-n\alpha - xe^{-\alpha}).$$

Thus

$$\sigma_N^A = \frac{\pi R^2}{n!}\,\gamma\left(n, \frac{A\sigma_{in}}{\pi R^2}\right). \tag{5.6}$$

TABLE I. Average number $\langle N\rangle_A$ of inelastic collisions in various nuclei. We have set σ_{in} equal to both 22 and 30 mb, appropriate for pions and protons, respectively.

A	r_{rms} (fm)	σ_{in} (fm^2)	$\langle N\rangle_A$
14	2.5	2.2	1.61
24	2.98	2.2	1.73
40	3.52	2.2	1.88
115	4.5	2.2	2.52
208	5.42	2.2	2.88
14	2.5	3.0	1.83
24	2.98	3.0	2.00
40	3.52	3.0	2.19
115	4.5	3.0	3.04
208	5.42	3.0	3.50

This is the final result for general values of A. However, there is a very interesting limit to this function. We know that $A/R^2 \sim A^{1/3}$. Thus the second argument of γ becomes large as A becomes large, and we can use an asymptotic form. We find to leading order

$$\sigma_N^A \underset{A\to\infty}{\sim} \frac{\pi R^2}{N} - \frac{\pi R^2}{N!}\left(\frac{A\sigma_{in}}{\pi R^2}\right)^{N-1} \exp\left(-\frac{A\sigma_{in}}{\pi R^2}\right). \tag{5.7}$$

This result is striking in that it shows that, for large A, σ_N^A becomes independent of σ_{in}. Thus for example σ_N^A is independent of the nature of the projectile, leaving the projectile dependence entirely within the excitation properties.

Finally, we shall give some numerical results for $\langle N\rangle_A$, using Eqs. (5.6) and (4.4), $\sigma_{in} = 22$ mb and 30 mb (appropriate for pion and proton projectiles, respectively), and values for R taken from electron scattering tables. Table I summarizes the results of this calculation. In addition, we plot $\langle N\rangle_A$ vs A on a semilog scale in Fig. 4. The heavy black points in this figure are the computed values of $\langle N\rangle_A$. For purposes of comparison we have drawn alongside the functions $\langle N\rangle_A = CA^{1/3}$

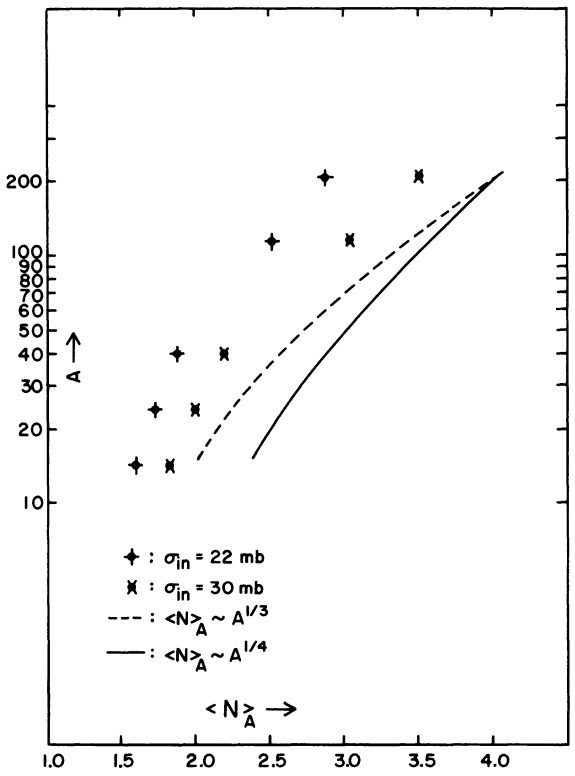

FIG. 4. Average number of inelastic collisions in a nucleus A, $\langle N\rangle_A$, plotted for $\sigma_{in} = 22$ and 30 mb. For comparison, the dashed and solid lines represent $\langle N\rangle_A = CA^{1/3}$ and $CA^{1/4}$, respectively.

(dashed line) and $\langle N\rangle_A = CA^{1/4}$ (solid line). Realistic nuclei seem to be described more accurately by the $A^{1/4}$ curve. With these values of $\langle N\rangle_A$ in hand, and some model for $\tau_M^{\text{projectile}}$, the distributions are completely determined.

VI. DISTRIBUTIONS

In this section, which is intended to be an experimental guide, we combine our results with some experimental input for the distribution of $p+p \to \pi^{\pm}+x$ to give distributions for $p+A \to \pi^{\pm}+x$. At 30 GeV the charged-pion single-particle distribution $\sigma_T^{-1} d\sigma/dx = f(x)$ as a function of the Feynman parameter x is well described[19] by

$$f(x) = 0.48 \exp(-7.4x^2) + 0.38 \exp(-12.1x^2). \tag{6.1}$$

In the neighborhood of $x=0$ ($|x|<0.15$) a scaling limit has not been reached, and at ISR (CERN Intersecting Storage Rings) energies the distribution is more accurately given by $f(x)+f(5x)$. For illustrative purposes we shall use Eq. (6.1); it is trivial to work out the second case. With $Q+R \approx 0.6$ and $\langle N\rangle_A$ given as in the previous section, Fig. 5 shows a plot in x space of the distribution $f_A(x)$ for various nuclei, according to Eq. (4.5). We have assumed that the multiply excited projectile distribution is identical with Eq. (6.1). Note also that the compression of the scale for $x<0$ varies as a function of A. The apparent discontinuity at $x=0$ is due entirely to the nonlinearity of the relation between x and the rapidity. In reality, the curve is not discontinuous and interpolates smoothly in rapidity. We would expect our result to be blurred in practice for the particles with the most negative x, because of the difficulty of escape for those particles produced nearly at rest with respect to the the nucleus.

To compute the average multiplicity one need only integrate the distribution over rapidity. With a definite model it is straightforward to perform the necessary integrals. However, the interpolation between zero lab rapidity ($x \lesssim 0$) and maximum lab rapidity (essentially $x \gtrsim 0$) requires knowledge of the multiple projectile excitation at its kinematic limit. Since maximum excitation mass and hence maximum multiplicity events populate the $x=0$ region, detailed calculation would be highly model-dependent. To get a reasonable estimate it suffices to interpolate linearly between the $r=0$ and $r=r_{\max}$ values. This procedure has the virtue that the integral can be analytically performed. We find

$$\langle n^{\pm}\rangle_A = \tfrac{1}{2}[\langle N\rangle_A (Q+R)+1]\langle n^{\pm}\rangle_H, \tag{6.2}$$

where $\langle n^{\pm}\rangle_H$ is the measured charged-pion multi-

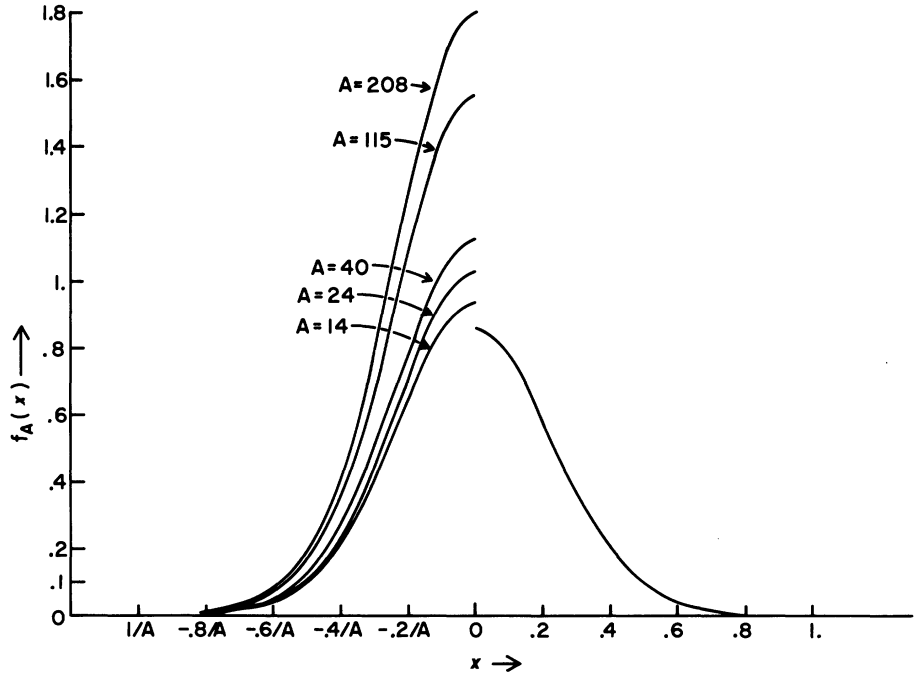

FIG. 5. Realistic scaling function for $p+A \to \pi^{\pm}+X$ on various nuclei. The function is taken from Ref. 19. The curve for $x>0$ is taken to be the input for the (symmetrical) reaction $p+p \to \pi^{\pm}+X$. Note the compression of the scale for $x<0$.

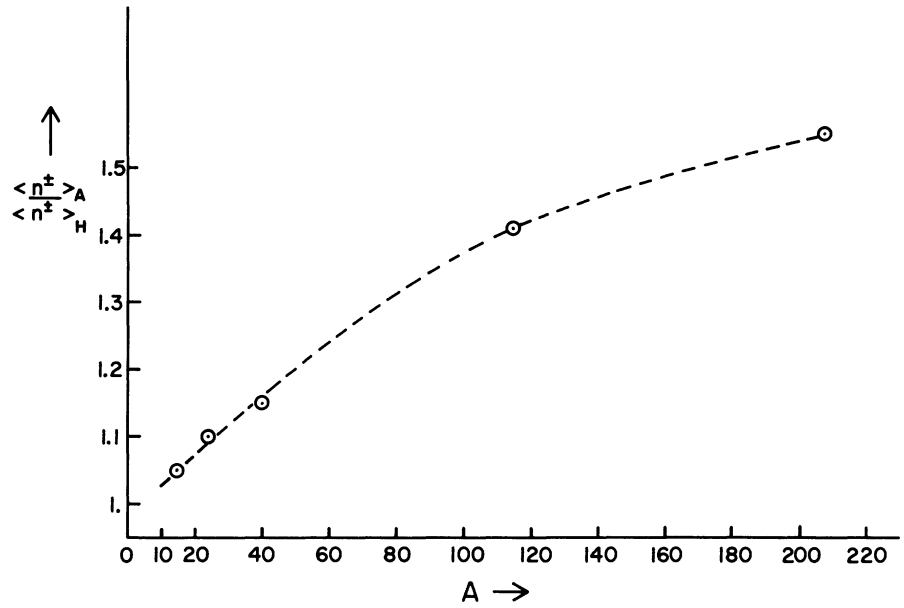

FIG. 6. Ratio of charged-pion multiplicity in $p + A \to \pi^{\pm} + X$ to multiplicity in $p + p \to \pi^{\pm} + X$, computed by integrating the distribution of Fig. 5 weighted with x^{-1}.

plicity in $p + p \to \pi^{\pm} + x$. In Fig. 6 we plot the ratio of $\langle n^{\pm} \rangle_A$ to $\langle n^{\pm} \rangle_H$. Of course, the logarithmic energy increase is retained. That the ratio is not enormous even for lead is a consequence of the size of $\langle N \rangle_A$, the number of mean free paths for inelastic collision. According to our previous discussion of $\langle N \rangle_A$, the ratio for realistic nuclei rises roughly as $A^{1/4}$. This sort of result has been observed previously[14] in the context of resonance excitation in nuclei.

ACKNOWLEDGMENTS

One of us (P. M. F.) wishes to thank Professor C. N. Yang for hospitality at the Institute for Theoretical Physics at Stony Brook and for helpful conversations on the topic of this paper.

---

*Work supported in part by The Research Corporation under a Cottrell Research grant; by the Center for Advanced Studies, University of Virginia; and by the National Science Foundation under Grant No. GP-32998X.

†Permanent address.

[1]P. M. Fishbane and J. S. Trefil, Phys. Rev. D 3, 238 (1971).

[2]A. Dar and J. Vary, Phys. Rev. D 6, 2412 (1972); L. W. Jones, in *Proceedings of the International Conference on Expectations for Particle Reactions at the New Accelerators, Madison, Wisc., 1970* (Univ. of Wisconsin Press, Madison, Wisc., 1970).

[3]W. Czyż and Lêsniak, Phys. Lett. 25B, 319 (1967); J. Formánek and J. S. Trefil, Nucl. Phys. B3, 155 (1967); J. S. Trefil, Phys. Rev. 180, 1366 (1969); 180, 1379 (1969); B. Margolis, Phys. Lett. 26B, 524 (1968); Nucl. Phys. B4, 433 (1968); K. S. Kolbig and B. Margolis, *ibid.* B6, 85 (1968).

[4]R. C. Hwa, Phys. Rev. Lett. 26, 1143 (1971).

[5]M. Jacob and R. Slansky, Phys. Rev. D 5, 1847 (1972).

[6]J. Benecke, T. T. Chou, C. N. Yang, and E. Yen, Phys. Rev. 188, 2159 (1969).

[7]D. Amati, S. Fubini, and A. Stanghellini, Nuovo Cimento 26, 896 (1962).

[8]G. Veneziano, Nuovo Cimento 57A, 190 (1968).

[9]P. M. Fishbane, J. L. Newmeyer, and J. S. Trefil, Phys. Rev. Lett. 29, 685 (1972); P. M. Fishbane, J. S. Trefil, and J. L. Newmeyer, Phys. Rev. D 7, 3324 (1973).

[10]P. M. Fishbane and J. S. Trefil, Phys. Rev. D 8, 1467 (1973).

[11]P. M. Fishbane and J. S. Trefil, Nucl. Phys. B58, 261 (1973).

[12]L. von Lindern, R. S. Panvini, J. Hanlon, and E. O. Salant, Phys. Rev. Lett. 27, 1745 (1971).

[13]T. K. Gaisser and R. H. Maurer, Phys. Lett. 42B, 444 (1972).

[14]J. S. Trefil and F. von Hippel, Phys. Rev. D 7, 2000 (1973).

[15]W. D. Walker, Phys. Rev. Lett. 24, 1143 (1969).

[16]Pythagoras, *The Quadrivium of Knowledge.*

[17]A. S. Goldhaber, C. J. Joachain, H. J. Lubatti, and J. J. Veillet, Phys. Rev. Lett. 22, 802 (1969);

C. Bemporad *et al.*, in *Proceedings of the Amsterdam International Conference on Elementary Particles, Amsterdam, 1971,* edited by A. G. Tenner and M. Veltman (North-Holland, Amsterdam, 1972).

[18]P. M. Fishbane, J. L. Newmeyer, and J. S. Trefil, Phys. Lett. 41B, 153 (1972).

[19]N. F. Bali, L. S. Brown, R. D. Peccei, and A. Pignotti, Phys. Rev. Lett. 25, 557 (1970).

PHYSICAL REVIEW D VOLUME 9, NUMBER 1 1 JANUARY 1974

Test of Cabibbo's model in hyperon semileptonic decays

Augusto García
Departamento de Física, Centro de Investigación y de Estudios Avanzados, Instituto Politécnico Nacional, Apartado Postal 14-740, México 14, D. F.
(Received 17 April 1973)

The experimental rates and angular correlation and symmetry coefficients are used to test Cabibbo's model in semileptonic hyperon decays. The data indicate that the one-angle model should be relaxed. We consider the possibility that $\theta_V \neq \theta_A$, and we investigate the influence of the q^2 dependence of the form factors. We find that the present data are sufficiently accurate to detect symmetry-breaking effects.

I. INTRODUCTION

The experimental evidence in hyperon semileptonic decays has increased lately, so that one can expect to have a better test of Cabibbo's model.[1] Previous recent tests[2-4] seem to favor the one-angle Cabibbo's model. Our present analysis aims at performing a more detailed test of this model and at investigating whether the current experimental evidence makes it worthwhile to consider symmetry-breaking corrections in semileptonic hyperon decays.

Instead of the experimental V/A ratios of the different decays, which have been used in the other tests, we prefer to use the available experimental angular correlation and asymmetry coefficients, because, otherwise, one would be losing information. In our opinion, this provides a more stringent test of the model.

In Sec. II, we review the parametrization in Cabibbo's model of the different hyperon semileptonic decays. In Sec. III, we use these parameters to fit the available data in this type of decays and we consider also the possibility that there be different vector and axial-vector Cabibbo angles. In Sec. IV we make some final comments.

II. PARAMETERS IN CABIBBO'S MODEL

We assume that the semileptonic decays of hyperons are all described by the $V-A$ theory, with time-reversal invariance, and electron-muon universality. For the internal-symmetry properties of these decays we take Cabibbo's model.[5] In the spirit of this model symmetry-breaking effects are assumed to be small enough to be neglected, except for the difference in the masses of the different hyperons. Also, only first-class currents are assumed.[6] The hadronic part of the transition amplitude is

$$\langle A|J_\mu|B\rangle = \left(\frac{M_A M_B}{E_A E_B}\right)^{1/2} \bar{u}_A(p')\left\{f_1(q^2)\gamma_\mu + f_2(q^2)\frac{\sigma_{\mu\nu}}{M_B}q_\nu + f_3(q^2)\frac{q_\mu}{M_B} + \left[g_1(q^2)\gamma_\mu + g_2(q^2)\frac{\sigma_{\mu\nu}}{M_B}q_\nu + g_3(q^2)\frac{q_\mu}{M_B}\right]\gamma_5\right\}u_B(p), \quad (1)$$

where B and A are the decaying and decay baryons, $J_\mu = V_\mu - A_\mu$, $q = p - p'$, and M_B is the mass of baryon B. According to Cabibbo's model, the form factors g_2 and f_3 can only contribute as symmetry-breaking effects. These effects are assumed to be small enough so that the contribution of these form factors can be neglected. For the electron-mode decays, the contribution of g_3 will be multiplied by the electron mass. Therefore it can be ignored, unless g_3 turned out to be unreasonably large. Since the range of variation for q^2 is small in all of these decays, the q^2 dependence of the form factors that contribute can be accounted for by keeping the linear term in a q^2 expan-